Supporting Information

Title: Targeted GSH-exhausting and Hydroxyl Radicals Self-producing Manganese-Silica Nanomissiles for MRI Guided Ferroptotic Cancer Therapy

Table S1 Drug loading capacity, drug entrapment efficiency, and antitumor property contrast between MMSNs@DHA and FaPEG-MMSNs@DHA.

	MMSNs@DHA	FaPEG-MMSNs@DHA
Drug loading capacity	28.23±2.95%	21.86±3.27%
Drug entrapment efficiency	13.58±1.23%	10.04±1.35%
Half-maximal inhibitory concentration (IC_{50})	13.90±1.74 μM	8.61±2.16 μM
In vivo tumor inhibition rate	65.60%	92.95%

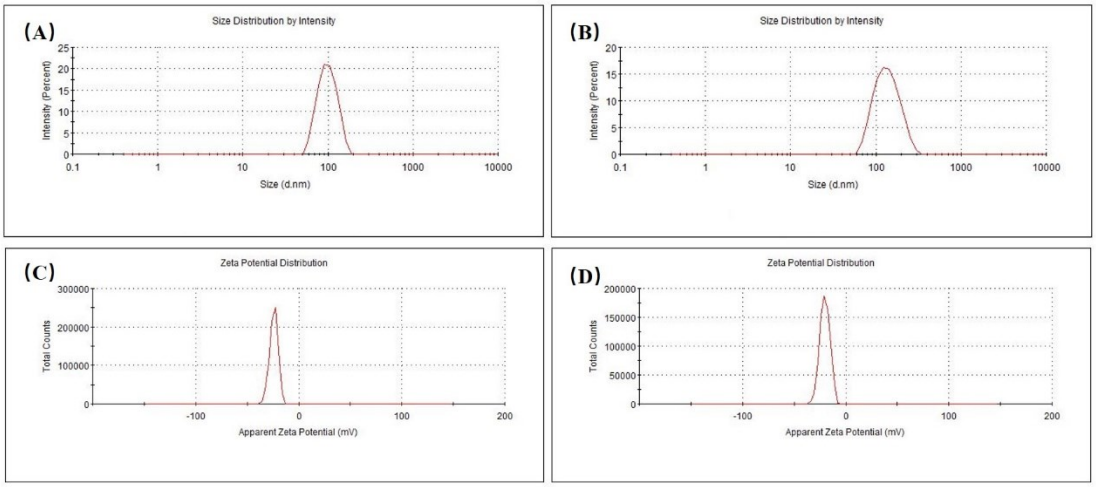

Fig. S1 Size and PDI distribution of MMSNs (A) and FaPEG-MMNSs (B). *Zeta*-potential of MMSNs (C) and FaPEG-MMNSs (D).

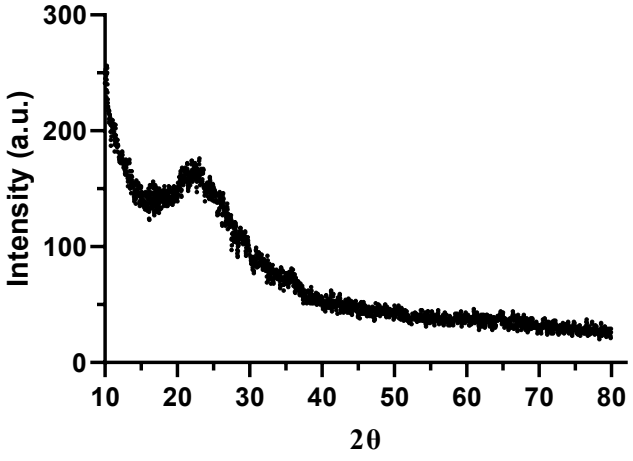

Fig. S2 XRD pattern of MMSNs.

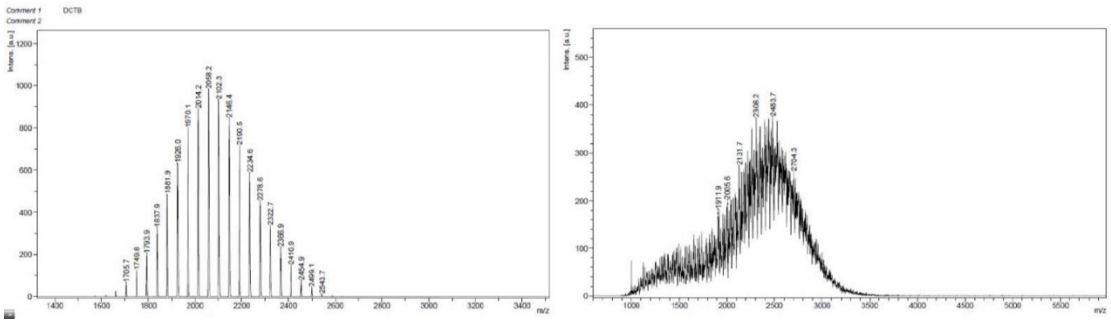

Fig. S3 MALDI-TOF-MS spectrum of PEG-silane and folic acid grafted PEG-silane (FaPEG-silane).

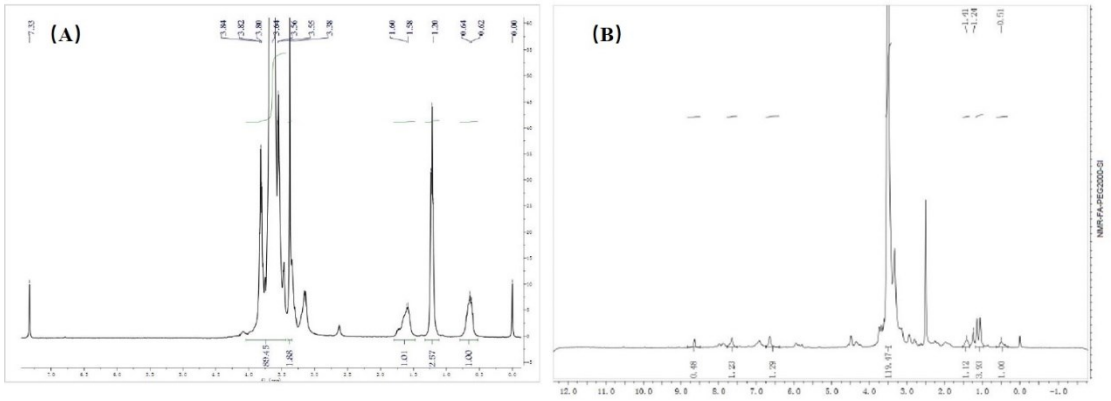

Fig. S4 ^{1}H-NMR spectrum of PEG-silane (A) and FaPEG-silane (B).

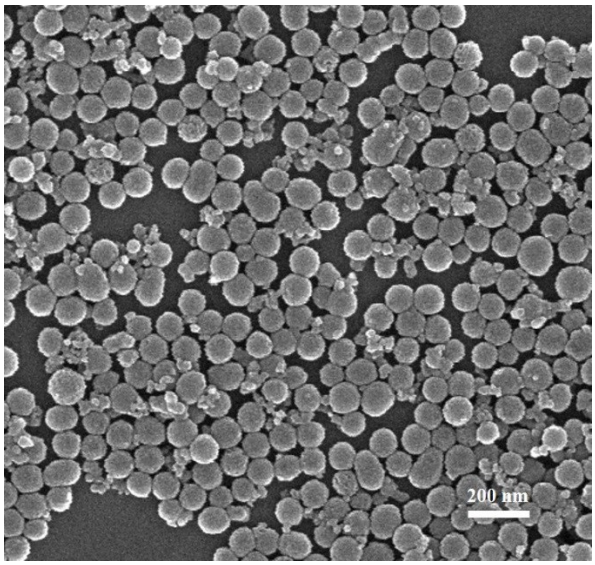

Fig. S5 SEM image of FaPEG-MMSNs.

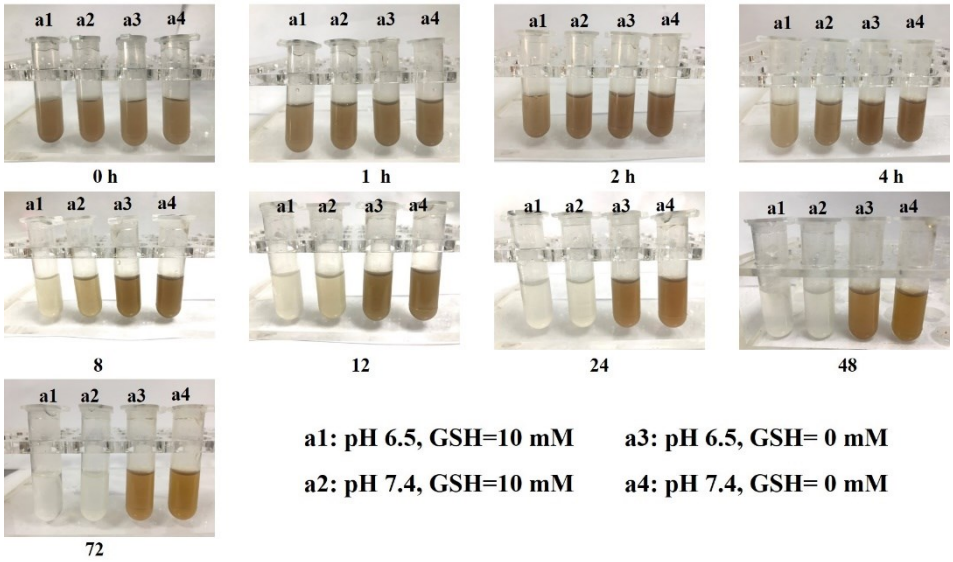

Fig. S6 Color changes of the dispersion during the degradation of FaPEG-MMSNs at different conditions.

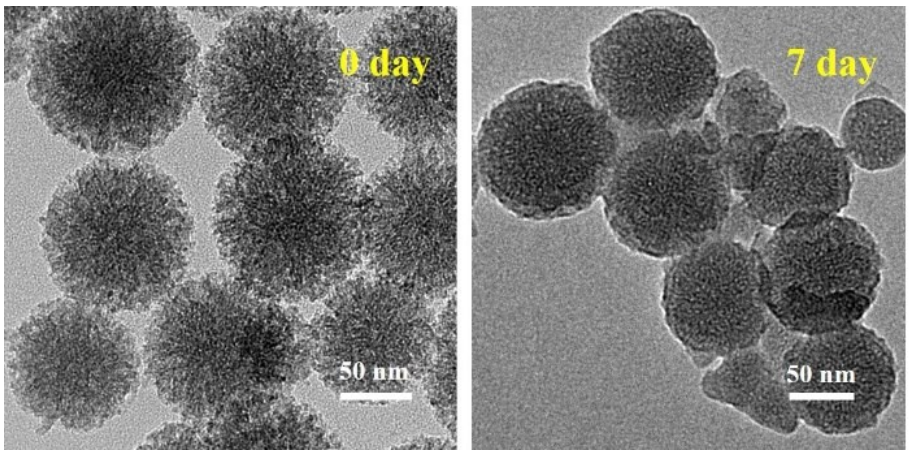

Fig. S7 *In vitro* degradation of FaPEG-MMSNs within 7 days under normal physiological condition (pH=7.4, [GSH]=0).

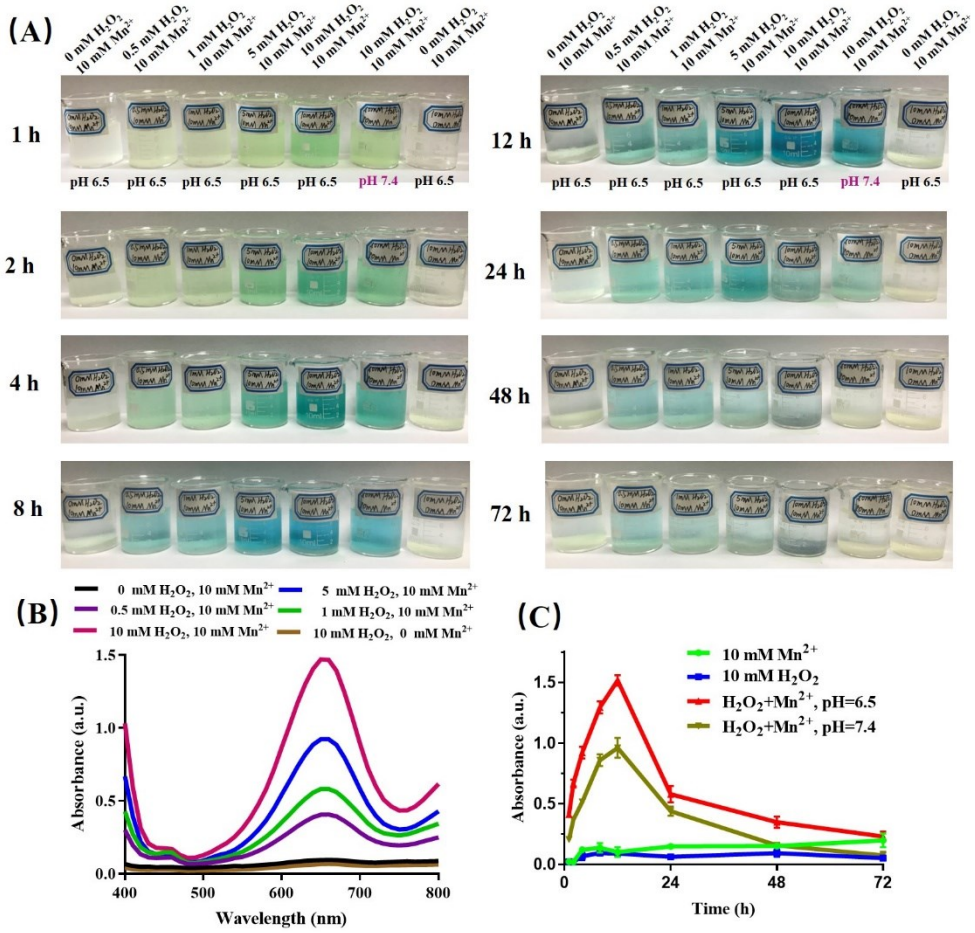

Fig. S8 TMB aqueous solution treated with different concentrations of H_2O_2 and Mn^{2+} for certain time (A). UV-vis spectra of TMB aqueous solution incubated with different concentrations of H_2O_2 in the presence of Mn^{2+} at 12 h (B). Absorbance changes of TMB aqueous solution incubated with different concentrations of H_2O_2 in the presence of Mn^{2+} at 650 nm during 72 h (C).

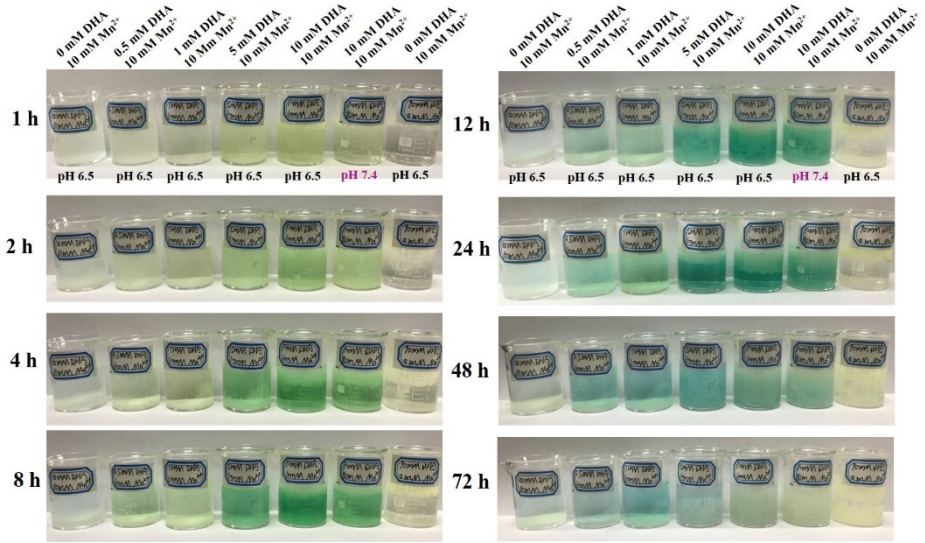

Fig. S9 TMB aqueous solution treated with different concentrations of DHA and Mn^{2+} for certain time.

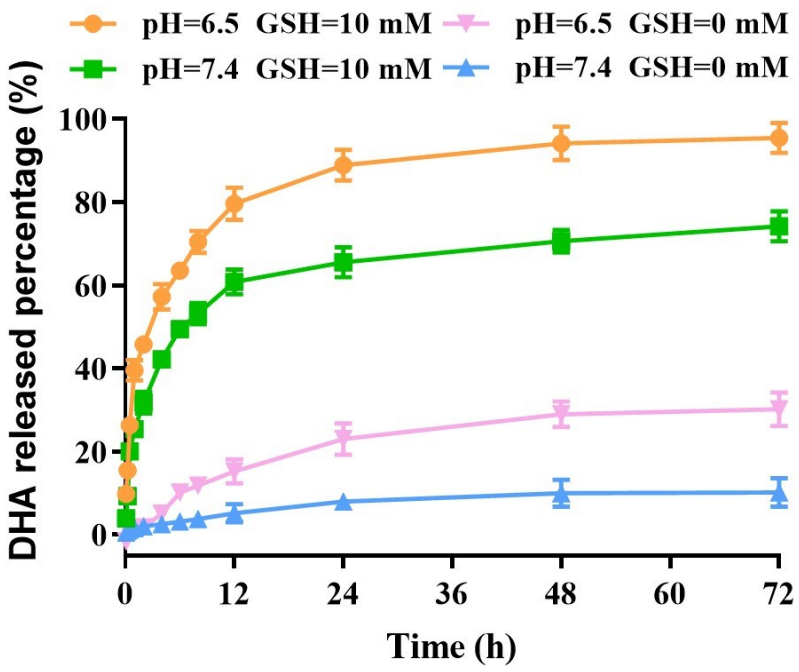

Fig. S10 Release profiles of MMSNs@DHA in buffers at different pH values and different GSH concentrations (n=3).

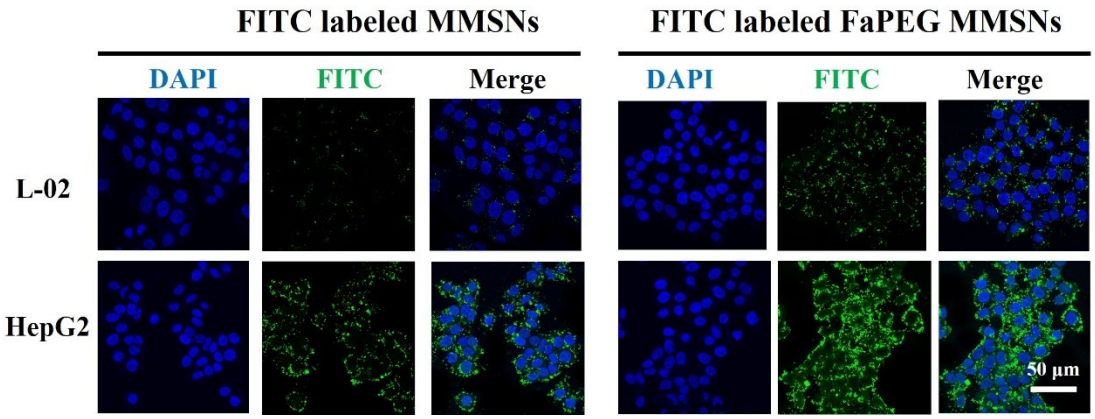

Fig. S11 CLSM images of HepG2 or L-02 cells after incubated for 4 h with FITC labeled MMSNs or FITC labeled FaPEG-MMSNs containing medium. The cell nucleus was stained with DAPI (blue).

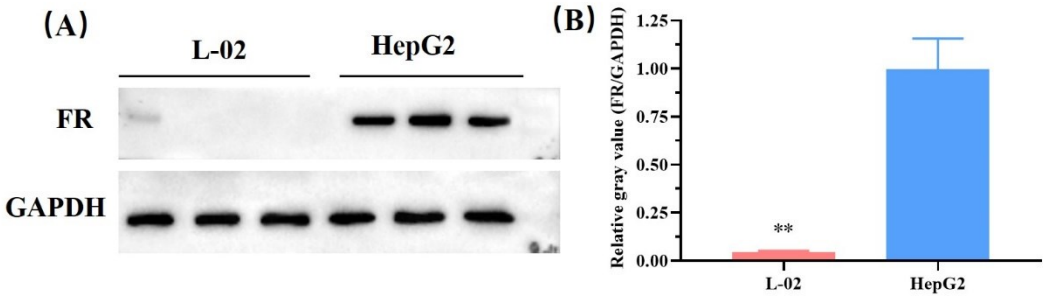

Fig. S12 Folate receptor (FR) expression of HepG2 and L-02 cells (A), Relative gray value (FR/GAPDH) of folate receptor in HepG2 and L-02 cells (n=3) (B).

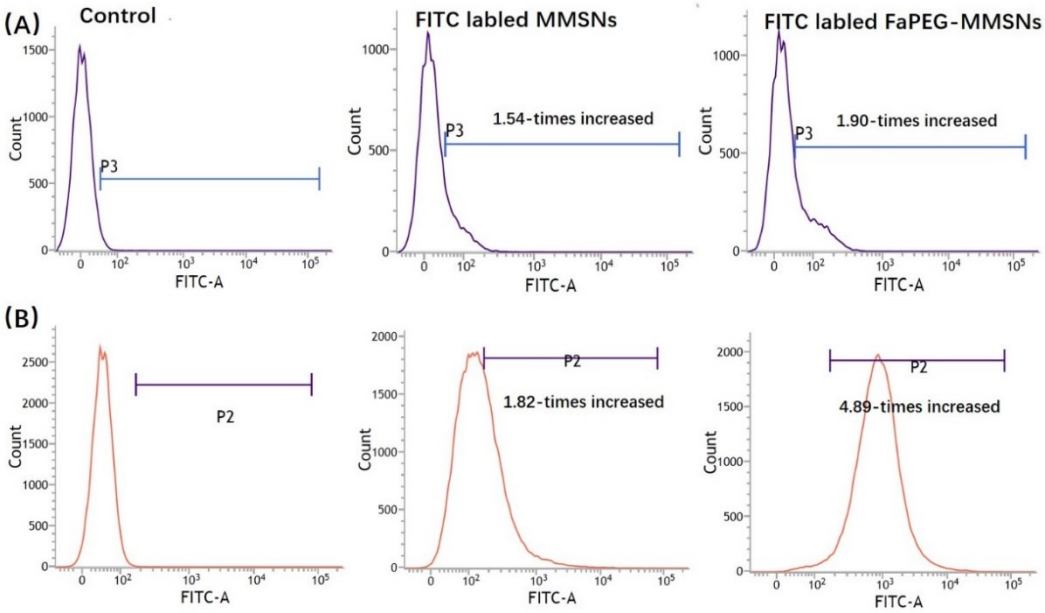

Fig. S13 Flow cytometry profiles of L-02 (A) and HepG2 (B) cells that were incubated with FITC labeled MMSNs or FITC labeled FaPEG-MMSNs containing medium (3 mM FITC per L) for 4 h.

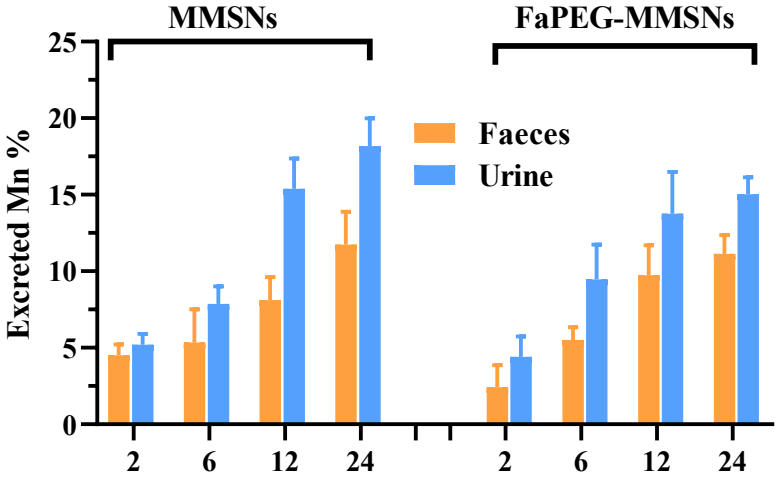

Fig. S14 Mn element excretion out of the mice body after the administration of MMSNs and FaPEG-MMSNs for different durations.

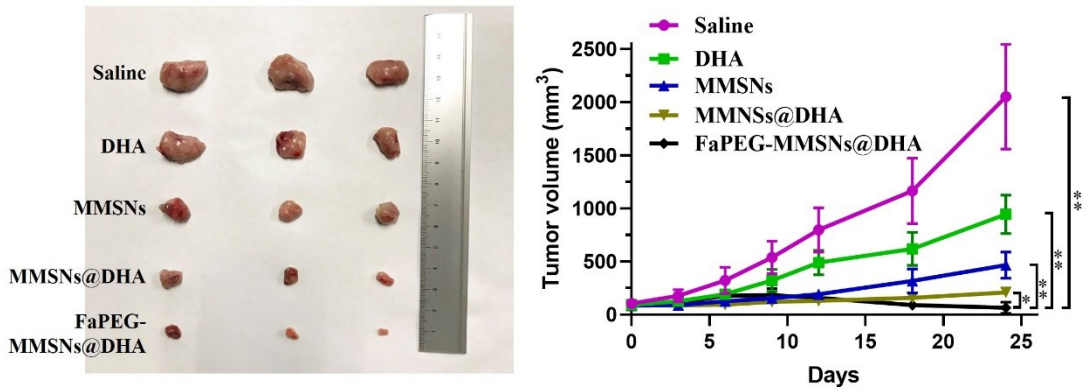

Fig. S15 The tumor photographs (A) on the day 24 (n = 3). Tumor volume curves (B) after intravenous injection of saline, free DHA, MMSNs, MMSNs@DHA, or FaPEG-MMSNs@DHA for 24 days. *$P < 0.05$, **$P < 0.01$.

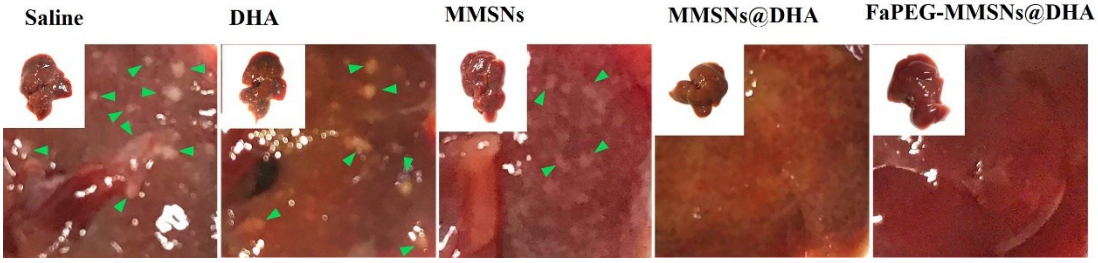

Fig. S16 Liver metastasis (white spots) of tumor after treatment with various formulations.

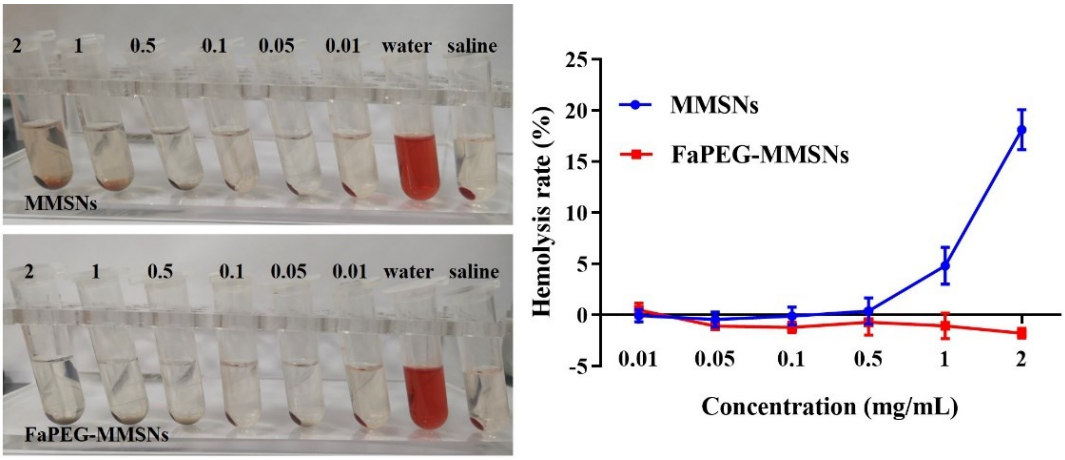

Fig. S17 Hemolysis properties of different concentrations of MMSNs and FaPEG-MMSNs.

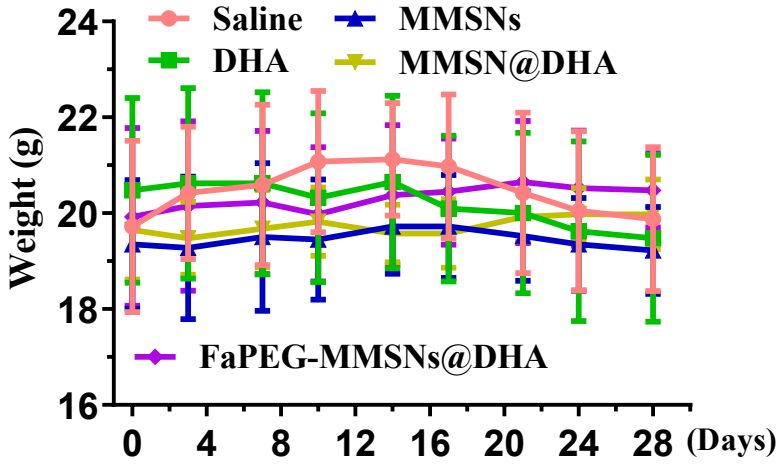

Fig. S18 Body weight changes of HepG2 tumor bearing mice over time during the treatment.

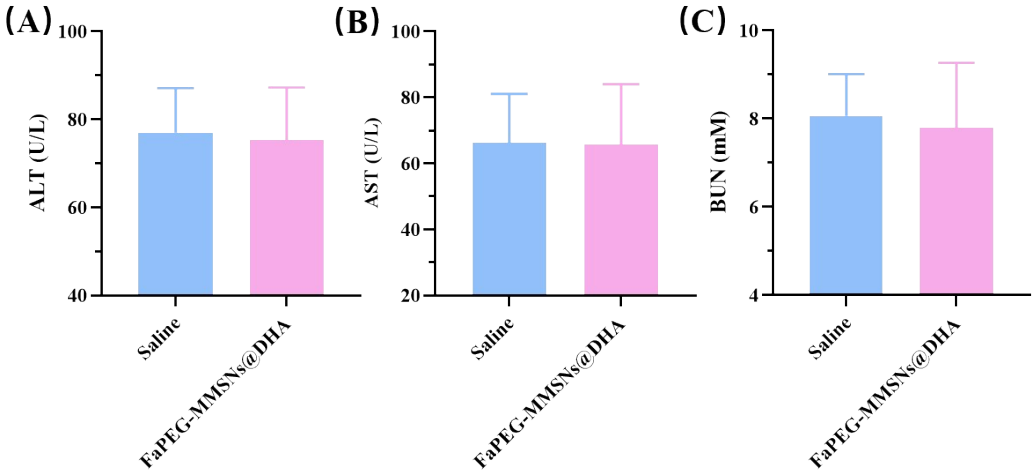

Fig. S19 Biochemical blood analysis of saline and FaPEG-MMSNs@DHA treated mice at 28 d post-injection. The terms include alanine aminotransferase (ALT) (A), aspartate aminotransferase (AST) (B), and blood urine nitrogen (BUN) (C).